Bulletin of the Seismological Society of America, Vol. 95, No. 5, pp. 1970–1987, October 2005, doi: 10.1785/0120040233

High-Resolution Satellite Imagery Mapping of the Surface Rupture and Slip Distribution of the M_w ~7.8, 14 November 2001 Kokoxili Earthquake, Kunlun Fault, Northern Tibet, China

by Yann Klinger, Xiwei Xu, Paul Tapponnier, Jérome Van der Woerd, Cecile Lasserre, and Geoffrey King

Abstract The M_w 7.8 Kokoxili earthquake of 14 November 2001, which ruptured a 450-km-long stretch of the sinistral Kunlun strike-slip fault, at the northeastern edge of the Tibet plateau, China, ranks as the largest strike-slip event ever recorded instrumentally in Asia. Newly available high-resolution satellite HRS images (pixel size ≤1 m) acquired in the months following the earthquake proved a powerful tool to complement field investigations and to produce the most accurate map to date of the coseismic displacements along the central Kusai Hu segment of the rupture. The coseismic rupture geometry south and west of Buka Daban Feng, near the earthquake epicenter, was also investigated in detail. Along the Kusai Hu segment, slip partitioning is for the first time observed to occur simultaneously during a single event, with two parallel strands, ~2 km apart, localizing almost pure strike-slip and normal faulting. In all, 83 new HRS coseismic offset measurements, some of which calibrated by field work, show large, well-constrained variations (≥100%) of the slip function over distances of only ~25 km. Tension cracks opening ahead of the shear dislocation and later offset by the upward propagating strike-slip rupture were observed, demonstrating that the rupture front propagated faster at depth than near the surface. The triple junction between the central Kusai Hu segment, the Kunlun Pass fault, where the rupture ended, and the Xidatan–Dongdatan segment, which could be the next segment to fail along the main Kunlun fault, acted as a strong barrier, implying that direct triggering of earthquake rupture on the Xidatan–Dongdatan segment by Kokoxili-type earthquakes may not be the rule.

Introduction

The M_w 7.8 Kokoxili earthquake of 14 November 2001 (also known as the Kunlun Shan earthquake [China Seismological Bureau, 2002]) was characterized by a fast eastward-propagating pulse of left-lateral slip (Bouchon and Vallée, 2003) that ruptured the Kunlun fault in northern Tibet (Figs. 1, 2) over a total distance of about 450 km (Xu *et al.*, 2002; Lin *et al.*, 2003; Antolik *et al.*, 2004). It is one of the largest continental strike-slip earthquakes ever recorded. Despite the efforts of several teams, the remoteness and high elevation of the fault and the great length of the surface break hampered exhaustive, systematic mapping of the slip along the surface rupture in the field. This rupture is often multistranded, which makes precise measurements of multiple coseismic offsets of clean piercing lines a formidable task. Hence, only partial and scattered measurements have been collected thus far. They provide a first-order shape of the slip function, but with limited detail and inconsistencies in several places (Lin *et al.*, 2002; Xu *et al.*, 2002). To document more thoroughly and quantitatively the slip and its variability along the rupture, we complemented our two field investigations by mapping the surficial breaks with recently available 1-m-resolution Ikonos and 60-cm-resolution Quickbird satellite images (later designated as high-resolution satellite [HRS] images) acquired after the earthquake. We present here the results of this work along a 100-km-long stretch of the main Kusai Hu segment of the fault (Fig. 2). Using this new tool, we are able to describe the full complexity of the surface rupture, and to obtain many measurements of coseismic displacements associated with the 14 November 2001 earthquake. The central part of the rupture was targeted for HRS image acquisition in the hours following the earthquake, since it became rapidly clear that it was the locus of the maximum amounts of coseismic slip (Kikuchi and Yamanaka, 2001; Xu *et al.*, 2002; Lin *et al.*, 2002, 2003; Antolik *et al.*, 2004). Our mapping illustrates a remarkable example of partitioning between coseismic strike-slip and

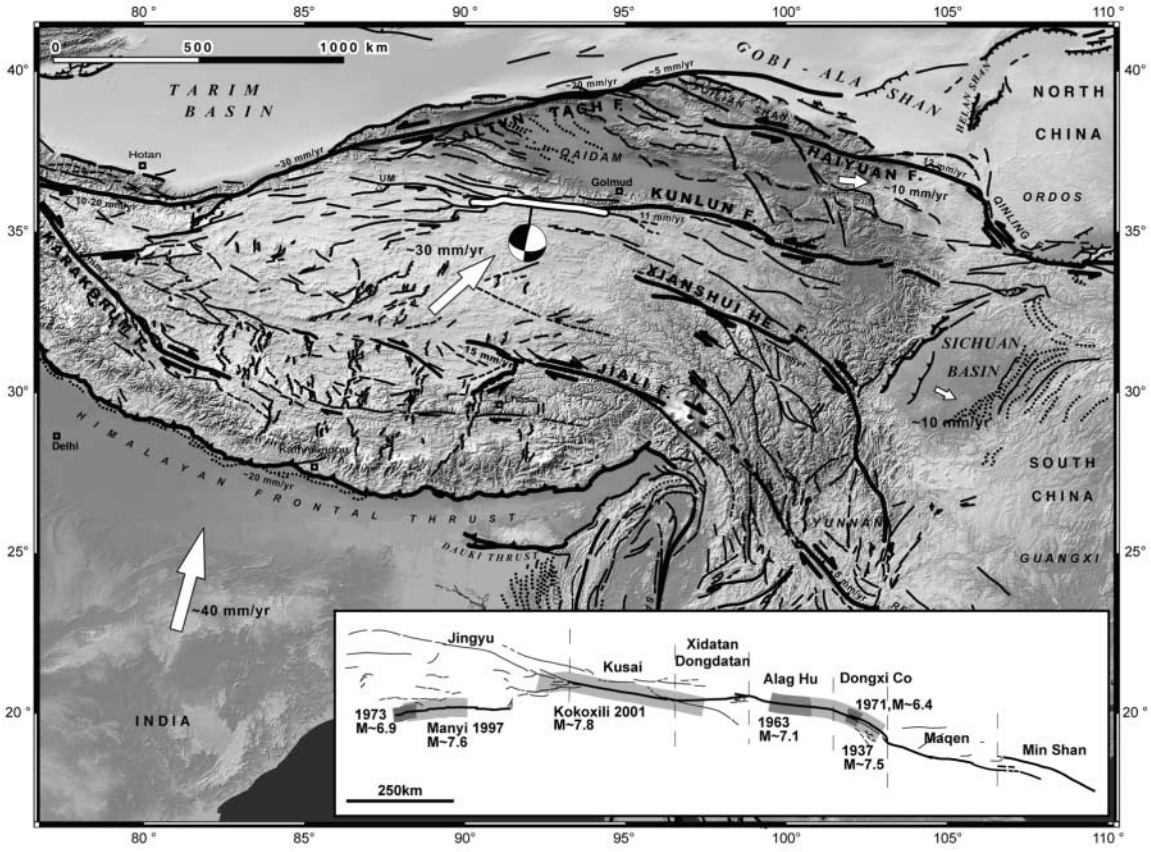

Figure 1. Main active faults of the Tibetan part of the India–Asia collision zone (modified from Tapponnier *et al.*, 2001). The 450-km-long rupture of the M_w ~7.8 Kokoxili earthquake (14 November 2001) is outlined in white, with centroid focal sphere (Harvard). The small triangle labeled UM is Ulugh Mustagh (7723 m). Inset shows earthquake dislocations along the Kunlun fault since 1930, emphasizing the very long rupture length of the 14 November 2001 earthquake and the seismic gap along the Xidatan–Dongdatan segment (different shades are used to distinguish between overlapping ruptures, modified from Van der Woerd *et al.* [2002b]).

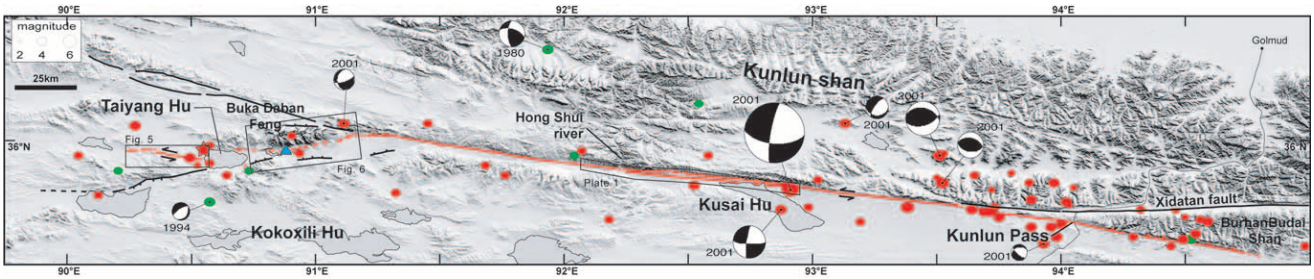

Figure 2. Rupture map of the Kokoxili earthquake. Earthquakes prior to 2001 are in green, aftershocks of the Kokoxili earthquake, in red (locations from NEIC). Focal mechanisms are from the Harvard database. For the Kokoxili main shock, the centroid moment tensor is shown. Red star, epicenter; blue triangle, hot springs. Places visited during fieldwork campaigns include areas described in Figures 5 and 6 and Plate 1, and the region east of the Plate 1 edge, as well as southeast of the Kunlun Pass.

Topography is from the Space Radar Topographic Mission (SRTM) database.

normal faulting along a 70-km-long subsegment of the rupture, and affords glimpses into the time history of vertical edge-dislocation propagation (Bowman *et al.*, 2003; King *et al.*, 2005). It also provides exceptional insight into the spatial, multiscale complexity of the seismic rupture.

Seismotectonic Setting of the Kokoxili Earthquake

Together with the Haiyuan, Altyn Tagh, Xianshui He, and Karakorum faults, the Kunlun fault is one of the main faults accommodating the present-day eastward extrusion of the Tibet plateau (Fig. 1) in response to the ongoing collision between India and Asia (Tapponnier and Molnar, 1977; Tapponnier *et al.*, 2001; Wang *et al.*, 2001). Seismic tomography studies suggest that such faults extend as shear zones deep into the mantle (Wittlinger *et al.*, 1998; Vergne *et al.*, 2002; Wittlinger *et al.*, 2004), localizing a large part of the lithospheric deformation. All of them have been sites of great earthquakes ($7.5 \leq M \leq 8.5$) during the past centuries (e.g., Gu *et al.*, 1989).

The Kunlun fault is about 1600 km long, extends from 86°E to 105°E, and strikes N100°E on average. Running along the south side of the Kunlun range, it follows the north edge of the high Tibet plateau (~5000 m above sea level [asl]). Based on dated offset geomorphic markers (Van der Woerd *et al.*, 1998, 2000, 2002b) and geodetic measurements (Wang *et al.*, 2001), the Kunlun fault has been shown to slip left-laterally at about 1 cm/yr on both decadal and millennial timescales. The main stretch of the Kunlun fault may be divided into six first-order segments delimited by geometric irregularities (Van der Woerd *et al.*, 1998). The westernmost horsetail of the fault comprises two segments, the Manyi segment to the south and the Jingyu segment to the north, splaying apart at Buka Daban Feng (also named Qinxing Feng) (Fig. 1, insert, [Van der Woerd *et al.*, 2002a]). The lengths of the different segments are variable, with rather linear segments over 200 km long, and shorter 100 to 150-km-long segments, separated by large-scale jogs or secondary splays. The Kusai segment, named for the largest lake it crosses, ruptured during the 14 November 2001 earthquake and is the longest rectilinear segment of the fault (270 km) (Fig. 2). To the west, the Manyi segment (Fig. 1) ruptured 4 yr prior to 2001, during the 1997 M_w 7.6 earthquake that produced a 170-km-long surface break with maximum offsets on the order of 7 m (Peltzer *et al.*, 1999; Velasco *et al.*, 2000). Farther west, magnitude ~7.3 earthquakes in 1973 had ruptured oblique, left-lateral faults, south of Ulugh Mustagh (Tapponnier and Molnar, 1977). In the east, two other segments of the Kunlun fault have ruptured since 1930: the Dongxi Co earthquake (35.5°N–97.5°E, 1937) (Fig. 1) with an estimated magnitude M ~7.5 (Jia *et al.*, 1988) reportedly produced about 150 km of surficial ruptures. Sinistral rill offsets of 4 m corresponding to this earthquake have been measured near the eastern end of that rupture (Van der Woerd *et al.*, 2000, 2002b). In 1963 an earthquake of estimated magnitude M ~7 occurred ~100 km west of Donxi Co, along the Alag Hu segment of the fault (Fig. 1), with reported surface offsets of several meters (Li and Jia, 1981). The focal mechanism was determined to be left-lateral strike-slip (Fitch, 1970; Tapponnier and Molnar, 1977). No large earthquake had been instrumentally recorded prior to 2001 along the Kusai Hu segment of the fault. The only significant instrumental events in the region are the M ~5.8 earthquakes in 1980 and in 1994, located 50 km north and 60 km south of the western end of the Kusai Hu segment, respectively (Fig. 2). The 1980 earthquake had a left-lateral focal mechanism with a significant thrust component. The fault plane solution of the 1994 earthquake, southwest of Buka Daban Feng, within the extensional horsetail of the fault, displays clear normal faulting on northeast-trending planes, in good agreement with mapped local active faults (Fig. 2) (Van der Woerd *et al.*, 2002b). East of the Kunlun Pass, between the 2001 Kusai Hu and the 1937–1963 Dongxi Co–Alag Hu ruptures, it seems that no large earthquakes occurred in the last 300 yr, at least on the Xidatan–Dongdatan segment of the fault (Fig. 1). This singles out that segment as the last one that might be close to failure between E92° and E103° (Van der Woerd *et al.*, 2002a; Xu *et al.*, 2002).

Methods

We reached the eastern end, the central Kusai Hu segment, and the western end of the rupture during two fieldwork campaigns in May 2002 and November 2003, respectively. At several places in these areas we measured, with a total station, clearly offset geomorphic piercing lines. Such measurements are accurate to within a few centimeters, the greatest source of error being the definition of the geomorphic features themselves. Because most of the markers are of natural, not man-made, origin, the greatest difficulty is usually to make sure that the offset features (rills, risers, etc.) are young enough to have been affected by one earthquake only. Inclusion of cumulative offsets of more ancient surface markers typically leads to unrealistically large last-event offsets (see differences between Lin *et al.* [2002] and Xu *et al.* [2002]). The main value of accurate total station measurements in the field is to provide solid quantitative ground truth. The drawback is that for a 450-km-long rupture, logistical constraints and fast scarp degradation dramatically limit the number of piercing lines sites quantifiable in this way.

To complement fieldwork, we used newly available HRS images to study and quantify the details of the rupture complexity. The HRS images (Ikonos and Quickbird) have a nominal pixel resolution of 1 m and 60 cm, respectively, and are thus at least 10 times more accurate than satellite images such as Spot, Landsat TM, or ASTER, which are commonly used in neotectonic studies. They allow detection of all cracks wider than ~0.5 m and measurement of minimum horizontal offsets of the same order (≥50 cm) (Fig. 3). In fact, for the first time, they make mapping of surface

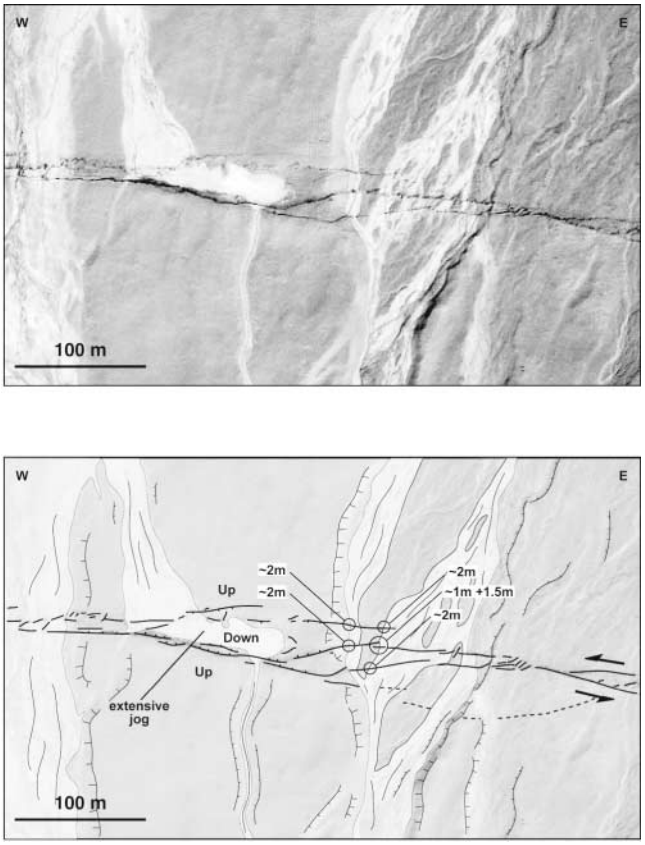

Figure 3. Example of mapping ground rupture with HRS images. Details down to ~50 cm are visible. The drainage network and terrace risers provide good piercing lines to measure sinistral offsets. Vertical throw along ruptures can only be estimated qualitatively from shading, stream capture, rupture geometry, surface deposition, erosion, and so on, as is clear for the small extensive jog. Location on Plate 1.

breaks of large earthquakes possible from optical space images. Plate 1 (unbound insert to this issue) shows the 100 × 5 km continuous swath of HRS images covering the central part of the Kusai Hu segment (Fig. 2) acquired after the 14 November 2001 earthquake. The strip map of the rupture derived from the HRS images, after georeferencing (Plate 1), shows most of the surface breaks that can be resolved on the images. Along with the detailed mapping of the rupture geometry, the HRS images are used to determine coseismic offsets associated with the November 2001 earthquake. To better assess measurement uncertainties, suitable measurement sites were cropped and resampled at 0.5 m/pixel. Stretching of the tonal response was used to increase contrast and clarity. Although we think that in most cases we can restore offsets to within 0.5 m, we conservatively take error bars on reconstructed offset measurements to be on order of ±1 pixel (±1 m). This technique not only rapidly provides a larger number of measurements compared with what can be achieved in the field, but also yields overviews of each piercing point site, limiting possibilities for erroneous mismatch (see the discussion of the Galway Lake Road offset measurements after the Landers earthquake in McGill and Rubin [1999] for a good example of this problem) and total station data projection problems due to local variation of the strike of the fault. Figure 4 illustrates the good match obtained at a site with measurements both in the field and with HRS images. Reconstruction of the beach lines on the HRS image yields an average offset of 5.5 ± 1 m (Fig. 4a and b), independently of who is performing the back-step restoration. Measuring the same features in the field leads to a comparable average horizontal offset of 5.3 m, validating the method (Fig. 4c and d). The slight difference (~10%) is due to a combination of factors: the difficulty in pinpointing the exact shape of the offset piercing line in the field, the poor definition of that line, the lack of perspective of the operator holding the staff, the variable width of the rupture zone, and the uncertainty in determining the exact angle to use to project total station profiles on the fault plane.

Outside the central Kusai Hu segment swath, other stretches of the rupture were later targeted for HRS image acquisition, but snow cover unfortunately hampered very detailed mapping and accurate offset measurements.

Geometry of the 2001 Kokoxili Earthquake Rupture

According to our observations, the November 2001 earthquake rupture appears to extend westward as far as ~90°15′E longitude. Besides rupturing the entire length of the Kusai segment of the Kunlun fault and part of the Kunlun Pass fault to the east (Figs. 1 and 2) (Lin *et al.*, 2002; 2003; Van der Woerd *et al.*, 2002a; Xu *et al.*, 2002), the earthquake dislocation broke the surface along a secondary strand of the fault, west of Taiyang Hu (Figs. 2 and 5). This is in keeping with the location of the instrumentally determined epicenter of the earthquake (National Earthquake Information Center [NEIC]), which is near the western shore of Taiyang Hu. The main dislocation then propagated eastward, reaching the Kusai segment of the fault through a series of oblique en echelon fault segments following the steep Southeast range front of the Buka Daban Feng. After fast propagation (Antolik *et al.*, 2004; Bouchon and Vallée, 2003) for about 270 km along the remarkably straight Kusai segment, the dislocation continued along the Kunlun Pass fault, leaving the Xidatan segment unbroken, to finally die off 70 km east of the Kunlun Pass (Fig. 2).

The following sections provide an overview, from west to east, of our mapping of the rupture, tied to the different styles of surface deformation we observed during our two field investigations, in May 2002 and November 2003.

West Taiyang Restraining Bend

We were able to trace the ground rupture westward to ~N35°57.6′, E90°16.2′ (Fig. 5, epicenter provided by NEIC: N35°57′, E90°32.4′), where it consists of only a few en echelon tension cracks. From that point eastward coseismic sin-

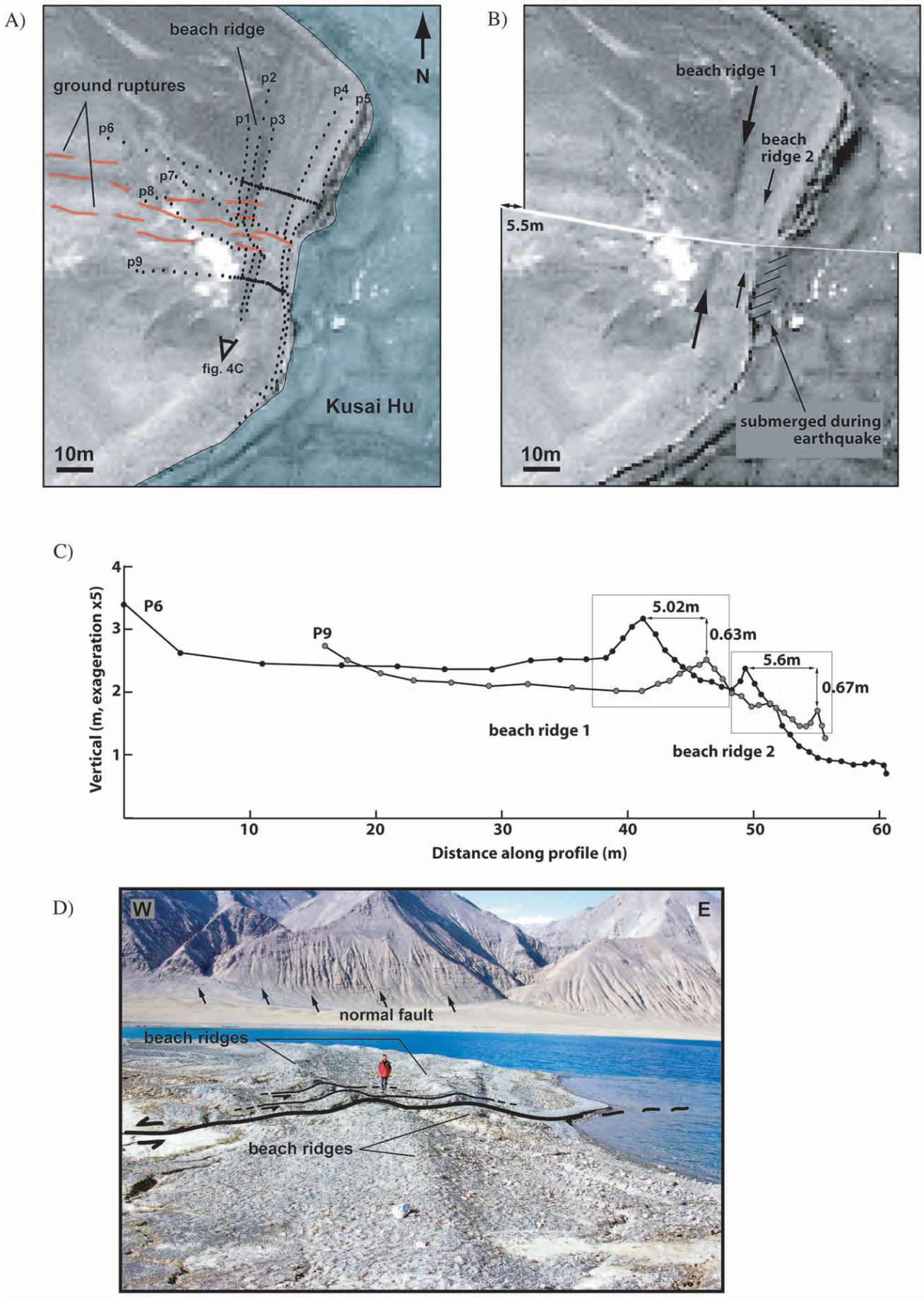
A)
beach ridge
ground ruptures
N
p1
p2
p3
p4
p5
p6
p7
p8
p9
fig. 4C
Kusai Hu
10m
B)
beach ridge 1
beach ridge 2
5.5m
submerged during earthquake
10m
C)
Vertical (m, exageration x5)
Distance along profile (m)
P6
P9
5.02m
0.63m
5.6m
0.67m
beach ridge 1
beach ridge 2
D)
W
E
normal fault
beach ridges
beach ridges

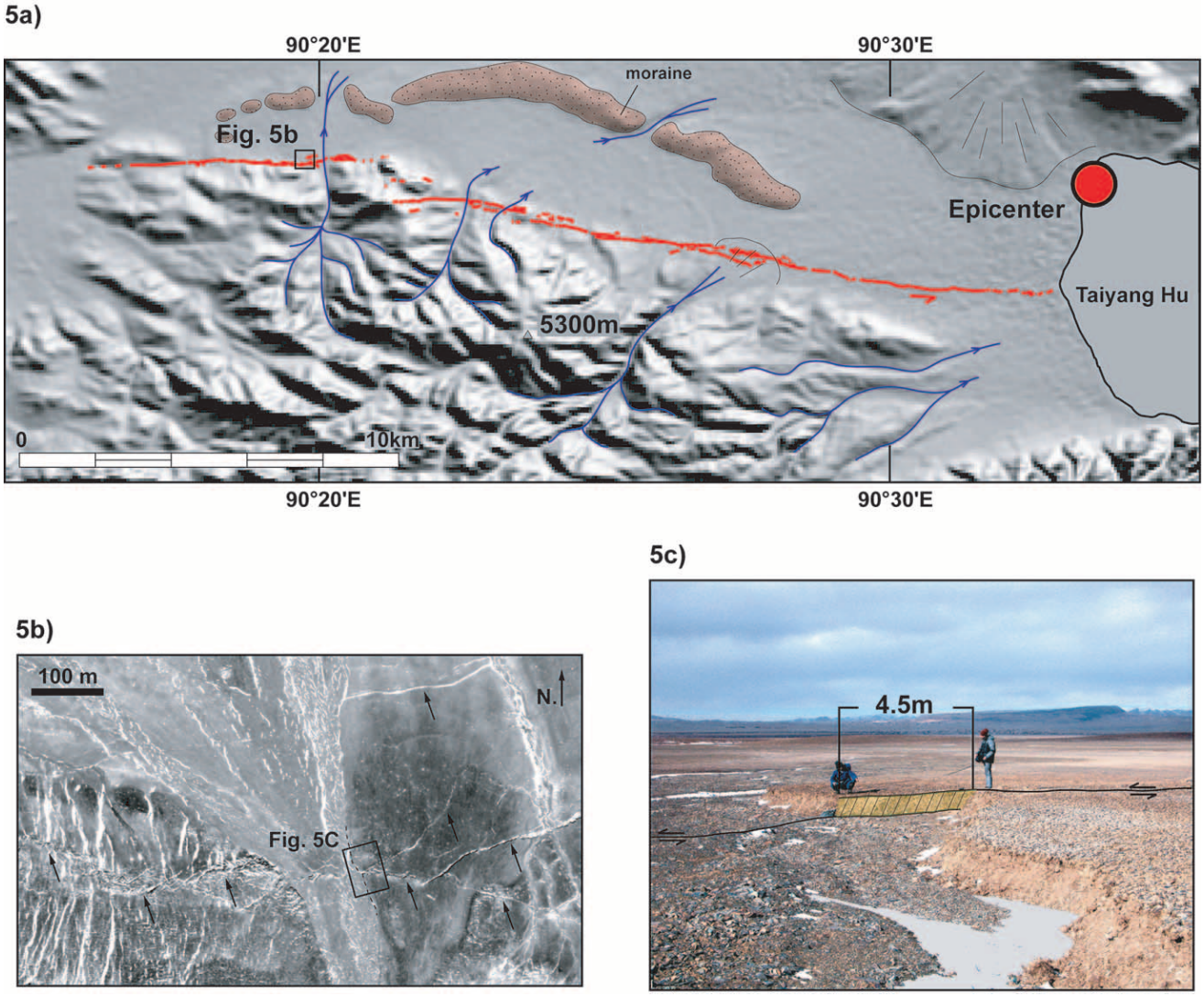

Figure 5. (a) Map of surface break west of Taiyang Hu, based on field observations and HRS images taken after the 14 November 2001 earthquake. Snow cover hampered systematic determination of accurate coseismic slip values. (b) Extract of HRS image showing ground rupture and the location of one clear 4.5-m terrace riser offset. (c) Field photograph of the 4.5-m terrace riser offset.

Figure 4. Offset of shoreline beach ridges east of large pull-part/push-up kink on the peninsula along the northern shore of Kusai Lake. (A) Profiles surveyed with the total station superimposed onto the HRS image. (B) 5.5-m retrodeformation of the shoreline to initial geometry before the Kokoxili event. (C) Projection of profiles 6 and 9 on the N102°E-striking plane, following the rupture zone. (D) Photograph, looking north, of offset beach ridges and of the range front normal fault, in background. Location on Plate 1.

istral slip increases rapidly, and the rupture takes the characteristic aspect of strike-slip surface breaks, with alternating pressure ridges and sag ponds. Few unambiguous coseismic offsets are clear in this flat area, however. We measured only one large unquestionable terrace riser offset (4.5 m at N35°57.6′, E90°19.8′, Fig. 5). At N35°57.6′, E90°21′, a 15° clockwise change of azimuth occurs, coinciding with a 1.4 km southward rupture jump and overlap. The strike of the rupture zone east of this bend is ~N110, close to the overall orientation of the Kunlun fault. The right-stepping overlap and restraining geometry of the bend suggest local shortening and folding within a 10-to 20-km long push-up (Fig. 5). East of the bend, the rupture remains within the mountainous terrain located south of the range front, and is discontinuous, with overlapping right-stepping segments typi-

cally 2 km long. The corresponding distributed deformation made unambiguous geomorphic offset measurements difficult. East of ~E90°25′, the rupture zone reaches back into the alluvial piedmont. We observed that only 2 yr after the earthquake coseismic deformation features had often already been almost completely washed out by the summer floods of seasonal streams. Elsewhere, the smoothed-out, cumulative relief of the fault scarp (down to the north, by about 1 to 2 m, much greater than that from the 2001 earthquake), however, indicates previous rupturing during the late Holocene. We could not trace the 2001 surface breaks to the Taiyang Lake shoreline in the field, but clear en echelon cracks may be followed to this shore on the HRS images (acquired earlier than our field campaign), attesting that the rupture did enter the lake. Careful inspection of the southern shoreline of the lake and of the southern edge of the sediment-filled trough south of the Buka Daban Feng show little evidence of coseismic 2001 surface rupture, with the exception of one short, completely isolated break (N35°53.4′, E90°42.6′) displaying mostly vertical throw, down to the north, over a distance of only a few hundred meters. Other well-smoothed-out scarps farther east likely correspond to older events.

Buka Daban Feng Oblique Normal Fault Corridor

The main fresh rupture zone likely comes back ashore along the northern side of Taiyang Hu. East of 35°57.4′ we mapped the 2001 break, with a down-to-the-south throw of 30 cm and a minor left-lateral strike-slip component that increases eastward. The broad alluvial fans that slope down from the range front to the small lake east of Taiyang Hu show large cracks oriented N108° on average, some with meter-wide opening. They probably formed as a result of spreading of the alluvial sediment apron toward the lake during intense seismic shaking.

The overall geometry of the earthquake rupture, which enters Taiyang Hu near its southwest corner and comes out of it near its northeast corner, indicates that the lake floods a pull-apart located within a left-stepping extensional jog of the Kunlun fault south branch. This rupture geometry, which is similar to that observed for the 1951 Damxung earthquake on either side of Beng Co Lake in southeast Tibet (Armijo *et al.*, 1989), implies that, given the location of the 14 November 2001 earthquake epicenter provided by NEIC (Fig. 2), rupture may have started within the pull-apart jog, a clear geometric asperity, and propagated eastward and westward, away from the lake (Lin *et al.*, 2003).

Below the main summit of the Buka Daban Feng range (Fig. 6), the main 2001 rupture zone is well developed, with en echelon subsegments striking N60° on average. The rupture crosses a hydrothermal field with hot springs aligned along it over a length of about 1.5 km (Fig. 7a). The rupture usually forms a dense array of en echelon fissures, with one stretch showing a prominent scarp with up to 1 m of left-lateral coseismic slip and several tens of centimeters of down-to-the-north throw. Cumulative deformation due to older events is clear. According to local eyewitnesses, hydrothermal outputs increased following the 2001 earthquake. The hydrothermal springs, already reported on geological maps, comprise many vents with surging hot or boiling water, but no H_2S. The freshly open fissures of the 2001 surface breaks also exhale water vapor. The origin of the heat cannot be assessed without heat flow measurements and subsurface investigation. While the hydrothermal vents are localized along the strike-slip surface rupture, they are also located within the extensional trough connecting the west Taiyang Hu and Kusai segments of the fault. This extensional corridor is bounded by very asymmetric range fronts, attesting to large differences in uplift rate (Figs. 2 and 6). A discontinuous front, well dissected in the east, characterizes the south side of the corridor, suggesting slow or incipient differential uplift, except west of 90.83°E. The maximum elevation is ~5500 m asl, only ~600 m above the trough floor (~4880 m asl). To the north, by contrast, steep triangular facets, more than 500 m high, bound the ice-capped Buka Daban Range (Fig. 6), which culminates at 6880 m asl, feeding eight large glaciers that pond in the trough. Large moraines and widespread till surround the toes of these glaciers. Six of them swing southwestward as they exit the range front, between the triangular facets, in a direction opposite to that of the overall, east-directed drainage of the trough. This westward swing may be due to channeling of the glaciers in a smaller graben following the range front, as suggested by the mountain-facing scarp located just east of the hot springs (Fig. 6). Sinistral offsets of the glaciers' lateral moraines are unclear, unlike those observed at glacial sites along other Tibetan strike-slip faults (Lasserre *et al.*, 2002; Meriaux *et al.*, 2004; Chevalier *et al.*, 2005). This may be due to the fact that, in the current interglacial, the glaciers still cross the range-front fault. Within the moraines at the base of Buka Daban Feng, evidence of surface rupture is unclear. Vertical motion may be distributed into numerous parallel or en echelon normal fault strands within the unconsolidated till, as suggested by the presence of multiple landslide head-scarps aligned along the moraine talus. Neither did we find unambiguous evidence for a fresh 2001 rupture at the base of the large triangular facets. Along the eastern part of the Buka Daban range front (Fig. 6), the 2001 rupture becomes more localized, with a clear south-facing normal scarp accommodating 1 to 2 m of throw, with a 1 to 1.5 m high free face (Fig. 7b). At places, a comparable amount of additional warping brings the total 2001 throw to 2 to 4 m. The horizontal slip component is not clear enough to be quantified. The area shows intense fissuring, with cracks over 30 cm wide. To the northeast, this prominent normal fault scarp meets with the Kunlun Shan range front, as the 2001 rupture bends clockwise by ~20°. It then follows this N105° striking front, resuming a predominantly strike-slip character. This sharp bend marks the western extremity of the Kusai Hu segment of the fault. That the 2001 earthquake epicenter was located in Taiyang Hu may account for

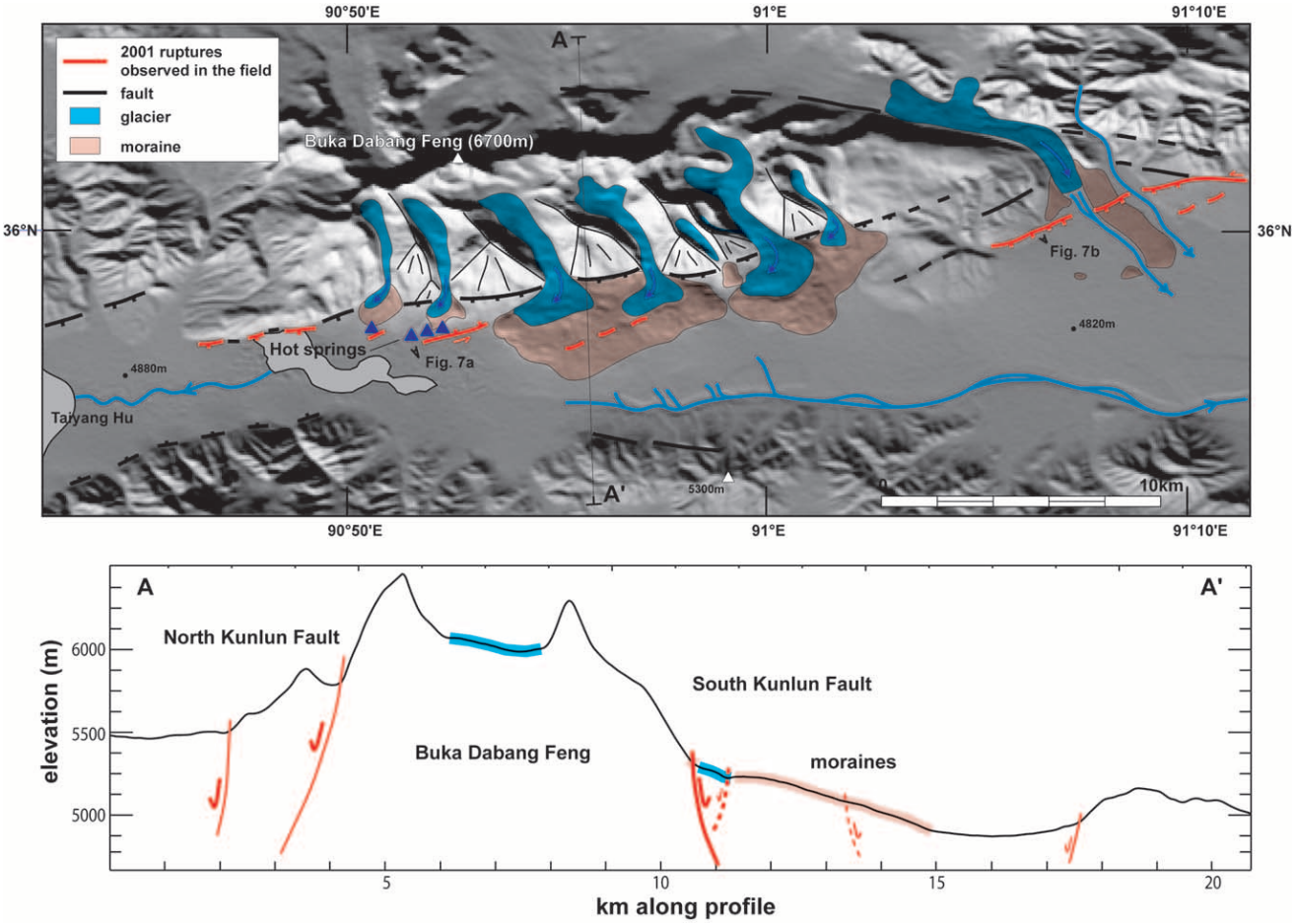

Figure 6. Map of extensional corridor south of Buka Daban Feng derived from field observations. The 14 November 2001 surface breaks are in red. Although field evidence for coseismic rupture along the range front fault was not found, or was ambiguous, overall morphology implies that it is active. Southwest deviation of glacier tongues is due to channeling in small range front graben. Hot springs (Fig. 7a) (blue triangles) are aligned along one strand that ruptured in 2001. Roughly north–south profile and cross section emphasize the asymmetry of the extensional corridor. Digital Elevation Model (DEM) is from the SRTM database.

the absence of rupture along the north branch of the western Kunlun fault, which is aligned with the Kusai Hu segment of the fault and continues to Jingyu Lake (Fig. 1 inset, Fig. 2).

Western Kusai Segment

For over 100 km eastward, the 2001 rupture zone is mostly single stranded, and exhibits nearly pure strike-slip motion. The presence of triangular facets near the western extremity of the Kusai Hu segment suggests, however, that some cumulative vertical throw is locally accommodated by the fault. This is a complex area, where the two main western branches (Jingyu and Manyi) of the Kunlun fault merge. At N35°52.8′, E92°13.8′ (Fig. 2, Plate 1) the Hong Shui River crosses the fault. It is the only drainage to breach northward across the Kunlun range to reach the Qaidam basin. West of this river, the rupture is rather simple with clear coseismic and cumulative offset of tributary fans and terrace risers. Both the fault trace and the 2001 surface break are sharp and well defined, making the area an ideal target to study the accumulation of displacement through several consecutive seismic cycles (Van der Woerd *et al.*, 2002b). Coseismic 2001 stream offsets of 3 ± 0.5m (Plate 1, Fig. 8), and cumulative offsets of 6 ± 1 m due to two successive earthquakes are measured both in the field and on the HRS images (Li *et al.*, 2005), suggestive of local characteristic slip (Klinger *et al.*, 2003; Liu *et al.*, 2004; Sieh, 1996).

Central Kusai Segment

The Hong Shui River gorge marks a second-order transition zone in the nature and style of faulting along the Kusai segment of the fault. At E92°14′, both the range front and the active fault zone slightly change azimuth, by about 3° counterclockwise, on average, and the Kunlun range front

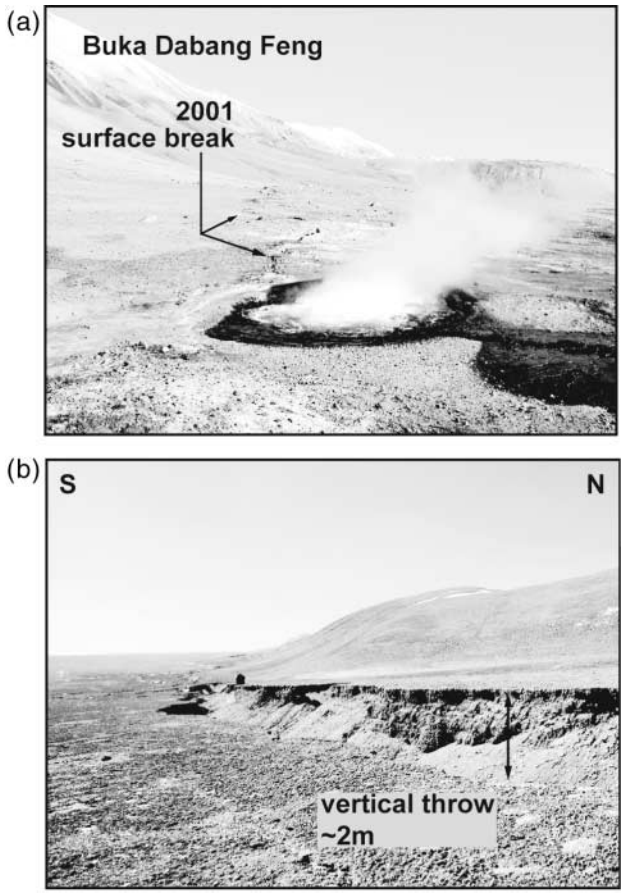

Figure 7. (a) View of boiling water in geyser pond in piedmont of Buka Daban Feng. Note hanging glacier pecten behind the moraine in the background. (b) The 2001 normal fault scarp at the eastern end of the Buka Daban Feng corridor (see location in Fig. 6).

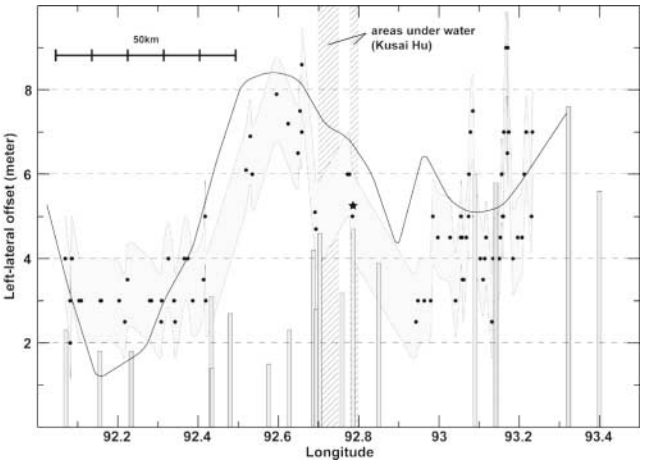

Figure 8. Horizontal slip distribution with 83 positioned offset measurements (Table 1) along the central part of the Kokoxili earthquake rupture derived from HRS images. Gray shaded envelope represents the nominal error of ± 1 m (see text for discussion). Star is shoreline measurement of Figure 4. For comparison, field data from Xu *et al.* (2002) are indicated by gray bars, and InSAR results from Lasserre *et al.* (2005) by the black line. Striped boxes locate Kusai Hu.

steps northward by about 1 km (Plate 1). This small releasing bend and step triggers partial to complete partitioning of the strike-slip and normal components of motion on two distinct, roughly parallel strands, one across the piedmont, the other along the range front, respectively, as already noted north of Kusai Hu by Van der Woerd *et al.* (2002a). The partitioned stretch of the Kusai Hu segment is about 70 km long, with a 30-km-long central part where the horizontal separation between the range front and the piedmont strands is nearly constant (2 to 2.5 km). In the west, this separation increases abruptly, in only ~2 km, to about 1–1.5 km. Then, past an abrupt kink of the parallel strands ~5 km eastward, it increases progressively over a distance of ~10 km to its maximum value of ~2.5 km. In the east, it decreases progressively, over a distance of about 20 km (Plate 1). Our field observations and detailed mapping using the HRS images (Plate 1) document the existence of fresh, coeval 2001 surface breaks along both strands, and, thus, for the first time, the occurrence of well-developed slip partitioning during a large earthquake. In related articles, we have suggested that the likely mechanical cause of such partitioning, and of the corresponding changes in near surface stresses, is the upward propagation of rupture (Bowman *et al.*, 2003; King *et al.*, 2005). The finite distance between the two strands is interpreted to reflect the depth at which the partitioning process starts and the two faults meet, likely where the oblique deep fault cuts across a rather shallow (a few kilometers deep) sediment/bedrock interface (Armijo *et al.*, 1986). Between E92°12′ and E92°56′, each ruptured strand is well defined and shows obvious signs of previous activation.

The range front, predominantly normal, fault strand follows the base of large triangular facets, several hundred meters high (Fig. 4d). The 2001 displacement due to the Kokoxili earthquake has produced free faces 1 to 2 m high, usually at the bedrock/colluvium contact. Nevertheless, parallel normal scarps cut the bedrock at places within the facet slopes. These scarps are unlikely to result from landsliding because they can be traced across several adjacent facets and alluvial fans. This leads to underestimation of the total normal throw, as measuring and integrating the throw across the upper scarps is impossible because of lack of access. Along the 70-km-long slip-partitioned stretch of the fault, the morphology of the 2001 normal escarpments varies. From the Hong Shui gorge to about 18 km eastward, these escarpments are fairly continuous. This is also the case in the east, along most of the 20-km-long stretch where the separation decreases northeast of Kusai Hu. Along much of the stretch of maximum strand separation, the normal escarpments are more discontinuous, and generally shorter. This probably reflects less efficient propagation of the normal dislocation all the way to the surface, due to the greater

depth of partitioning. Indeed, there is no hint, whether on HRS images or in the field, of diffuse deformation along the range front. Concurrently, it is also in this central part of partitioned rupture (E92°36′ to E92°52′) that multiple normal fault scarps cut the fan and terrace surfaces in the intervening zone between the normal and strike-slip fault strands. Some such scarps show fresh 2001 surface breaks, particularly just north of the western extremity of Kusai Hu and at E92°26′ (Plate 1), but several others do not, even though they are large and easy to map on the HRS images. Most of these intervening scarps have a characteristic geometry in map view (Plate 1). They start close to the main strike-slip strand, with a markedly oblique azimuth (30° to 40° counterclockwise from E100°) that swings progressively northward to become parallel to the main normal strand along the range front. We interpret such a systematic azimutal swing to reflect the transition between the two superficial partitioned stress regimes in the zone where none of them is adequate to promote the formation of long-lived fault planes with steady-state kinematics (see figure 3 in King *et al.*, 2005).

The strike-slip strand is located well south of, and several tens of meters down below the range front. Along most of its length it shows little evidence of vertical motion (Plate 1). One exception is the 4-km-long stretch between E92°28′ and E92°30′, near the western end of the maximum separation zone, where a range-facing scarp developed, blocking and diverting the drainage. Although this scarp might result from apparent vertical throw due to cumulative sinistral shift of higher and older fans north of the fault to the west, shuttering younger deposits, the youthfulness of the surfaces south of the fault and very large amount of left-lateral transport required (on the order of 5 to 6 km) make this hypothesis unlikely. Vertical motion along this segment in the 2001 Kokoxili event was small enough, however, that it did not significantly dam the one large stream that continues to flow in the channel incised across the cumulative scarp.

Another area where the piedmont strand kinematics departs from pure strike-slip faulting is where it encroaches upon Lake Kusai (Fig. 2, Plate 1B). The northern shore of this lake, which lies mostly south of the fault zone and has a shape that does not suggest a simple tectonic origin, is cut four times by the fault (Plate 1). One notable pull-apart basin (Fig. 9a and b), contiguous with a push-up hill of similar size to the east, formed in the promontory near N35°49.2′, E92°46.2′. Two more pull-apart sags may be present under water on either side of this promontory. The onshore pull-apart is about 1000 m long, 200 m wide, and 20 m deep. All the normal faults bounding its floor slipped in 2001, with 1.9 m of vertical offset on the south side and about 1 m on the north side (Fig. 9a and b). One fault strand, taking up most of the 2001 strike-slip displacement, shortcuts the basin along its longest diagonal. Deformation due to the 2001 earthquake has led to upthrow and the consecutive abandonment of the pre-2001 depocenter in the lower part of the basin floor (Plate 1, Fig. 9a and b). We found no piercing line in the basin that was clear enough to constrain the horizontal 2001 coseismic offset, but several rills at the base of the push-up slope a few hundred meters eastward provided a set of consistent measurements indicating ~5 m of sinistral slip (Plate 1, Fig. 8). The offset beach ridges east of the pull-apart basin also show consistent 5 to 5.6 m lateral offsets (Fig. 4). The existence of the two other pull-aparts in the lake bays east and west of the promontory may be deduced from the fault geometry. Extensions of the rupture traces offshore show large enough misalignments that they require the presence of ~200-to 500-m-wide extensional steps beneath the lake waters. On the HRS images and in the field, we mapped dense arrays of northeast-striking cracks parallel to the lakeshore in the two areas where the rupture enters the lake from the west (Plate 1, E92°42′). Such cracks might be attributed to spreading, but because they are not as numerous elsewhere, we suspect they are due in part to the existence of the underwater extensional pull-apart jogs. The sudden counterclockwise change of azimuth of the surface rupture before it enters the lake from the east in the eastern bay, which is associated with growing vertical throw, also argues for this interpretation.

East of Kusai Lake, the strike-slip rupture zone is up to 30 m wide with parallel strands bearing clear traces of large previous events (Fig. 9c). Fresh pressure ridges, cracks, and extensional pull-aparts are superimposed on older similar features, such as extensional sag ponds still marked by grassy mats and fine, buff-colored silt deposits reflecting water stagnation prior to the 2001 earthquake, and meters-high mounds covered by shattered and weathered ground with exhumed cobbles long exposed to the harsh high-altitude climate. This indicates that the rupture localization is stable through time, and hence, that slip partitioning along the two strands is likely a permanent type of coseismic behavior that repeats itself in successive earthquakes along this stretch of the fault.

For the next 12 km eastward, between the lake and the junction of the piedmont and range front strands, the strike-slip strand is sinuous but simple. The range front strand, on the other hand, is more complex along the first half of this distance. There is also one prominent ~1200-m-long, intervening crack array in the piedmont. Outside this array, however, there is little evidence for oblique ruptures trying to connect the two strands. The eastward tapering area in between is in fact remarkably crackfree. At E92°57′ longitude, the two strands merge into a single fault zone, located at, or a few hundred meters south of, the mountain front.

Eastern Kusai Segment

From that point eastward, the rupture pattern becomes more complicated, even though full partitioning is not observed. The fault zone becomes up to 400 m wide at places. It is often composed of parallel, or oblique en echelon, kilometer-long subsegments (Plate 1). This geometry makes it more difficult than elsewhere to measure the total coseis-

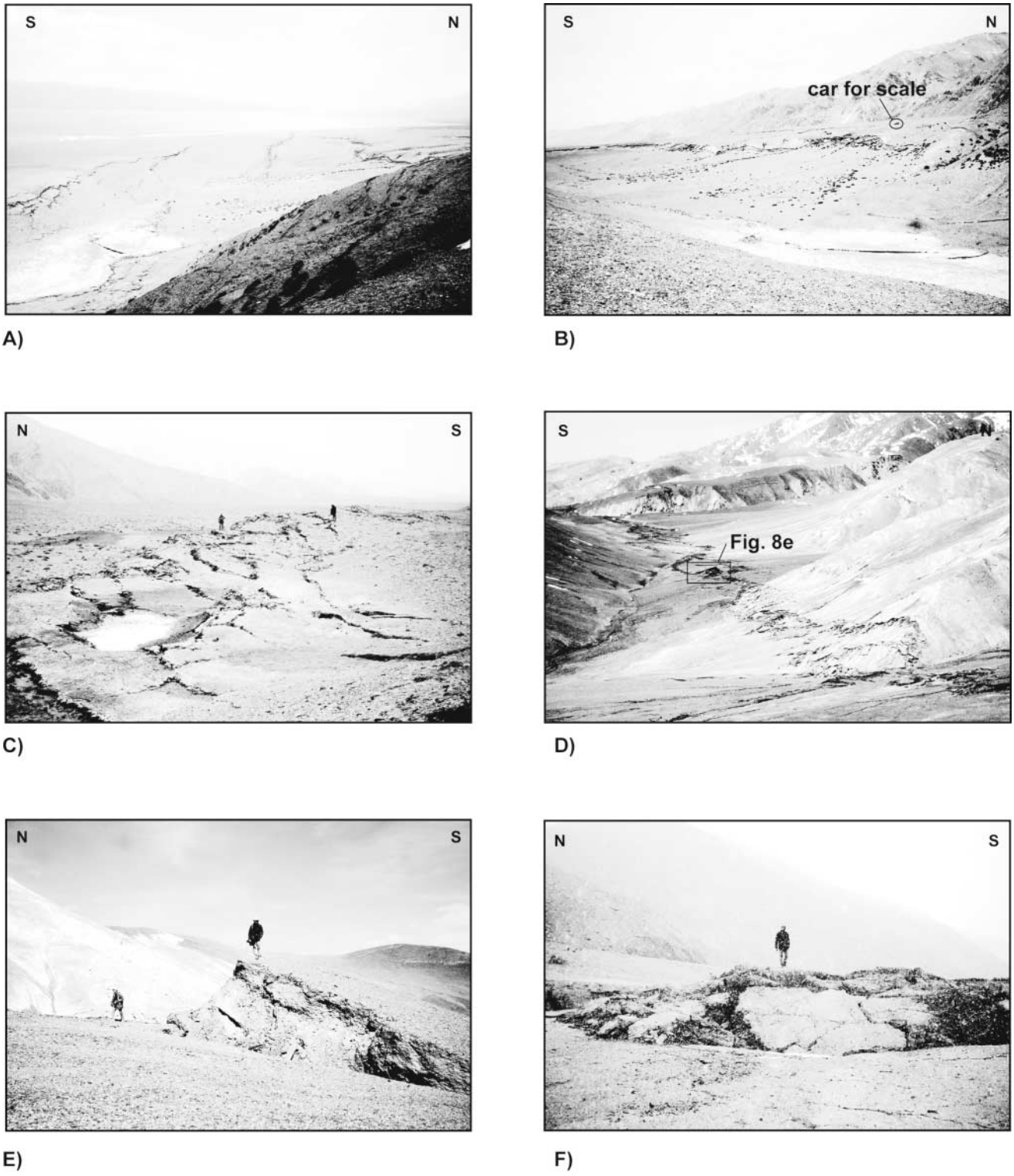

Figure 9. (A) General view of the pull-apart basin on the Kusai Hu peninsula. Normal motion is localized on the sides of the basin. The rupture in the center of the basin takes most of the strike-slip component. (B) View of the reactivated normal fault scarp on the northern side of the basin. (C) Evidence of repetitive, analogous earthquake rupture pattern along the piedmont fault trace. New sag pond created by the Kokoxili earthquake (water-filled, white on photo) formed within an ancient degraded sag created by an earlier large event (permanent, green-yellow grassy mat and fine, buff-colored silt) (D, E and F) Examples of ground rupture related to permafrost: 5-m-high pressure ridge is entirely bounded by brittle faults, including a large thrust that has tilted the intact ground surface. Location on Plate 1.

mic offset across the fault zone, which is distributed over distinct subsegments. As apparent from the disparate results of several studies of the earthquake, this is the section where the exact amount of coseismic displacement is most debated, even though it appears to be largest (Antolik *et al.*, 2004; Lasserre *et al.*, 2005; Lasserre *et al.*, 2003; Lin *et al.*, 2002, 2003; Xu *et al.*, 2002). Our total station measurements in the field and offset restorations on the HRS images confirm that the largest 2001 coseismic slip did not exceed 10 m along the section we studied in greater detail (Fig. 8). Due to the combination of multiple rupture strands, large horizontal displacements, and the presence of permafrost, this section offers some of the most spectacular surface deformation features (Fig. 9d, e, and f). At places, the frozen ground hampered surface folding, promoting instead brittle faulting and block tilting (Lin *et al.*, 2004). On Figure 8e and f, for instance, the intact upper surface of the west limb of a ~5-m-high push-up was lifted and tilted by ~30°. This implies decoupling of a rigid surface layer on a shallow thrust ramp, allowing the broken upper ground slab to rotate freely. Large plates of relatively unconsolidated, but frozen, alluvium are often observed to stand on end, in precarious equilibrium. Similar features have been documented for other large earthquakes in similarly extreme environments (Armijo *et al.*, 1989; Allen *et al.*, 1991; Haeussler *et al.*, 2004). In two deep valleys where fluvial incision exposes rocks beneath the Quaternary alluvium veneer, we observed that two parallel rupture strands followed the outer limits of a steep zone of black gouge, several hundred meters wide, separating the phyllonites and schists of the Kunlun range basement from the folded, south-dipping Tertiary red beds of the piedmont. The separation of the two strands is thus both of structural and mechanical origin. In the same area, ancient moraine ridges are offset by up to 2.5 km (Plate 1), suggesting sustained displacement since at least the late Pliocene at the current rate of ~1 cm/yr (Kidd and Molnar, 1988; Li *et al.*, 2004; Van der Woerd *et al.*, 2002b).

Kunlun Pass Fault Segment

Near N35°43.8′, E93°39′, the 2001 rupture abandons the main trace of the Kunlun fault, which follows the Xidatan and Dongdatan troughs (Fig. 2) (Van der Woerd *et al.*, 1998, 2001, 2002b). No coseismic rupture is observed along the Xidatan-Dongdatan segment of the fault, though subtle signs of ground distortion and possibly cracking are perceptible, in the west, on the HRS images and on the InSAR data (Lasserre *et al.*, 2005). Given the acquisition date of the images, such deformation traces could testify to postseismic creep. For 5 to 7 km, near E93°65′, the 2001 rupture shows short, northeast-directed splays indicating that it might have tried to jump to the Xidatan strand, without success. East of E94°, the rupture becomes linear and simple, following the trace of the Kunlun Pass fault at the foot of the Burhan Budai Shan (Kidd and Molnar, 1988; Van der Woerd *et al.*, 2002b), extending southeastward for another 70 km (Xu *et al.*, 2002). For most of its length, the Kunlun Pass fault surface break is limited to one single strand with almost pure strike-slip motion. At the Kunlun Pass, the 2001 coseismic displacement has been accurately measured by different teams to be ~4 m (Lin *et al.*, 2002; Xu *et al.*, 2002). East of the Golmud–Lhasa road (N35°40.2′, E94°3′), and south of the Burhan Budai summits (Fig. 2), a thrust component is observed locally in the field, accommodating 1–2 m of displacement in addition to the strike-slip component. Both slip components taper eastward in amplitude, to become limited to open cracks parallel to the fault near the rupture end (Xu *et al.*, 2002). This observation is hardly compatible with seismic inversion results, which require 4 m of surface slip at the eastern end of the rupture to account for the seismic waveforms (Antolik *et al.*, 2004). Rather, the surface slip decreases slowly over a long distance, which is in keeping with a dogtail type of rupture termination such as defined by Ward (1997).

Insight on Rupture Propagation from Surface Break Observations

The way seismic rupture propagates during an earthquake is an important topic of ongoing research (Bhat *et al.*, 2004; Rice *et al.*, 2005). It remains difficult to bridge theoretical models, laboratory experiments, and observations from large magnitude earthquakes owing to scaling problems. Inversion of seismic waves recorded by seismometers and accelerometers adequately images broad-scale dynamic rupture propagation along the fault plane (see, for this earthquake, Antolik *et al.*, 2004; Bouchon and Vallée, 2003; Ozacar and Beck, 2004; Rivera *et al.*, 2003 and, more generally, e.g., Peyrat *et al.*, 2001), but typical frequencies used in these studies are ill adapted to resolve details of the rupture history.

In both laboratory experiments and natural outcrops (Tchalenko, 1970), brittle faulting generally starts by an array of en echelon tensile cracks, the direction of the array being parallel to the future fault plane (e.g., Tapponnier and Brace, 1976; Scholz, 1990). Such tensile cracks are thought to ultimately coalesce into a brittle shear zone usually marked by a layer of gouge. HRS image and field mapping suggest that these two stages exist in the formation of a single earthquake rupture. Figure 10 shows two locations where the surface rupture pattern is characterized by one principal strand. The rather linear strands cross cut and offset gullies and terrace risers. At both locations, large en echelon cracks oriented northeast–southwest, in keeping with sinistral strike-slip motion, are also visible. None of them can be traced continuously across the strike-slip rupture. The opening component of the cracks must be greater than 50 cm to be visible on the images. Restoration of the offset gullies and risers by back-slipping one side of the fault relative to the other (by 7 m at one site and 4.5 m at the other), also restores the alignment of several cracks across the strike-slip rupture. Comparable observations were made along the 1968

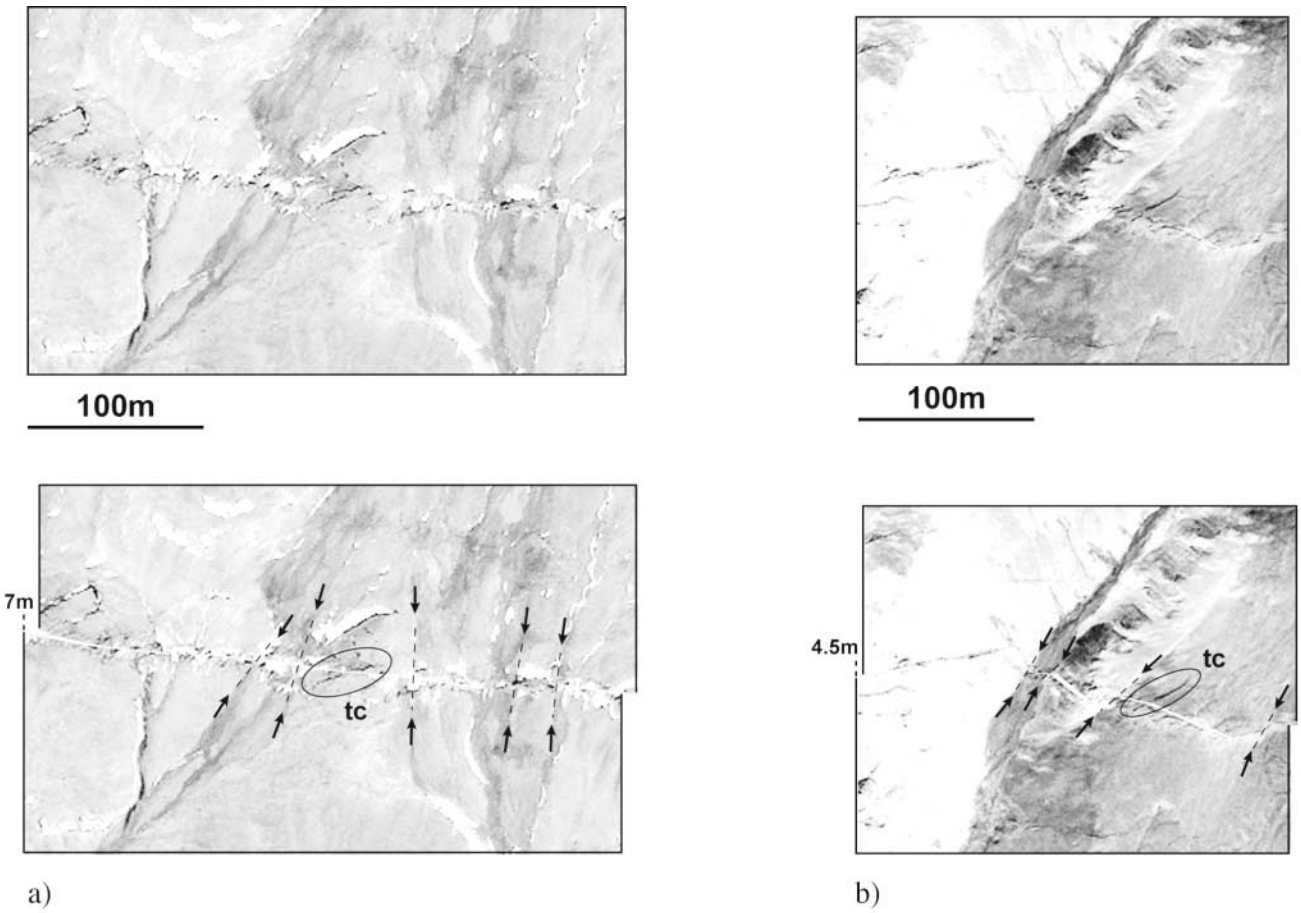

Figure 10. Reconstruction of offset tension cracks. (a) Left-lateral offset of 7 ± 1 m. (b) Left-lateral offset of 4.5 ± 1 m. Arrows indicate stream channel piercing points. Back-slipping realigns oblique tension cracks (tc), implying that they have been offset by more localized horizontal shear after opening. (c) Field photograph of tension crack offset by subsequent horizontal shear. Location on Plate 1.

Dasht-e-Bayaz earthquake surface break in Iran (Tchalenko and Ambraseys, 1970), a 24-km-long stretch of which was mapped in particularly great detail in the field and with air photos. Such examples show unambiguously that the cracks from first and are sheared only later. Such cross-cutting relationships support the inference that an en echelon crack damage zone propagates ahead of the shear rupture, whether in screw or in edge mode. This zone moves at the speed of the dynamic stress field generated by the rupture (King *et al.*, 2005), causing tensile cracks to open first, particularly at the stress-free ground surface. When the shear plane reaches the surface, it cuts and offsets the tensile cracks. In the last few meters, tensile cracking may be enhanced by the existence of unfaulted sediments deposited after the penultimate earthquake. This scenario is in keeping with a slip-partitioning mechanism involving upward propagation, with a rupture velocity much faster in the crust at depth than in the shallow, poorly consolidated sediments up above. A similar phenomenon is observed in analog experiments where a sheared clay layer is wetted at the surface by a water film (Tapponnier and Varet, 1974).

Horizontal Slip Distribution along the Central Segment of the Kokoxili Earthquake

Surface mapping of the coseismic slip distribution along the 14 November 2001 Kokoxili earthquake rupture zone is particularly challenging owing to the remoteness and great length of the surface break. Selected spots have been targeted for accurate field surveys (Li *et al.*, 2004; Lin *et al.*, 2002; Xu *et al.*, 2002), but most teams have reached different localities, which makes cross-checking of the measurements difficult. Taking advantage of the unprecedented resolution provided by the HRS sensors, we provide here additional measurements along the central stretch of the Kusai segment by systematically realigning piercing lines visible on the images (see Figs. 3, 4, and 10 for typical examples of offset restoration). One should bear in mind that telling the difference between cumulative offsets and 2001 coseismic displacements, which is not always straightforward in the field, often remains difficult on the images, even with a nominal 1 m pixel. We were able to measure a total of 239 offset features over a length of ~100 km. Among the 239 offset measurements, we eliminated all the data for which piercing points were ambiguous or for which the offset could arguably be considered as cumulative from the 2001 Kokoxili event and the penultimate event. This procedure yielded 83 reliable 2001 offset measurements (Fig. 8, Plate 1 and Table 1). The main uncertainty in the measurement is then simply related to the pixel size (~1 m). Therefore, we take the nominal error bar to be ± 1 m even though it is probably smaller. The resulting slip distribution pattern can readily be compared to that obtained by other groups or with other techniques. In the west, over a length of ~30 km, surface slip is nearly constant, with an average value of ~3 m. This value is validated in the field at Hongshui Gou (Li *et al.*, 2005). Between E92°24′ and the western shore of Kusai Hu, even though data is more limited, in part due to the north-facing scarp damming the drainage (Plate 1), the slip increases regularly to a maximum value of ~8 m around E92°42′. This is a stretch with well-established partitioning and no significant extensional jog. The few onshore data points farther east, which include our total station field measurements, confirm that the slip decreases back to 4-5 m. East of E92°54′, the slip increases again to a maximum value of 9 ± 1 m, accurately measured on two nearby offset geomorphic features at E93°6′. The whole data set reveals two relative maxima in the surface slip function, one at ~8 m, the other at 9 m, about 30 km apart. Field studies (Xu *et al.*, 2002) and InSAR data (Lasserre *et al.*, 2005) suggest that the largest amount of coseismic slip along the entire rupture, ~10 m, is located 10–20 km east of the area targeted with the HRS images, a region covered with snow at the time of image acquisition. Thus, the eastern slip function maximum in Figure 8 should in fact be seen as part of an increasing ramp toward the actual maximum. But the comparison with other data sets (Fig. 8) shows that our HRS measurements are generally in keeping with slip functions found with alternative techniques, particularly with InSAR. The field measurements of Xu *et al.* (2002), which tend to underestimate the total slip and should thus be regarded as lower bounds, nevertheless fit adequately with the HRS data in the west and east. The slip peak of ~8 m centered at ~E92°36′, on the other hand, does not show up in the field data of Xu *et al.* (2002), while it is quite clear in the InSAR results derived from the study of Lasserre *et al.* (2005). Since the slip function derived from seismic-wave inversion (Antolik *et al.*, 2004) was forced to be consistent with the data of Xu *et al.* (2002), where available, it is not surprising that it also misses the E92°36′ slip peak. The fit between the InSAR results and the HRS data set, which is quite good on average, indicates that most of the surface deformation is localized. Otherwise displacements measured by InSAR would be systematically larger than the surficial offset data. Such localized, shallow slip is confirmed by seismic inversions, which locates the largest slip patches above 5 km depth (Antolik *et al.*, 2004; Ozacar and Beck, 2004; Rivera *et al.*, 2003). All the data sets also show that coseismic slip increased eastward, in keeping with east-directed rupture propagation (Bouchon and Vallée, 2003; Le Pichon *et al.*, 2003; Rivera *et al.*, 2003; Antolik *et al.*, 2004).

Discussion

As one of the largest shallow continental earthquakes ever recorded, the 14 November 2001 Kokoxili earthquake provides a unique opportunity to study rupture processes in the continental crust. Using new metric-resolution satellite images, with local fieldwork calibration, we have been able to produce accurate maps of the surface break of this earth-

Table 1
Measures of Displacements from HRS Images (See Also Plate 1)

Longitude	Offset (m)	Longitude	Offset (m)	Longitude	Offset (m)	Longitude	Offset (m)
92°4′8.04	4	92°23′11.76	3	92°59′5.28	5	93°9′2.16	4
92°4′51.96	3	92°24′48.6	3.5	92°59′49.92	4.5	93°9′10.8	4.5
92°4′53.76	2	92°25′3	5	93°1′40.08	4.5	93°9′21.96	6
92°5′5.64	4	92°25′8.4	3	93°2′28.68	3	93°9′30.96	5
92°5′9.96	4	92°31′10.2	6.1	93°3′14.4	4.5	93°9′35.64	5
92°6′12.96	3	92°31′48	6.9	93°3′17.64	5	93°9′42.12	7
92°6′32.04	3	92°32′6.36	6	93°3′26.64	4.5	93°10′0.48	9
92°9′23.4	3	92°35′43.8	7.9	93°3′31.68	3.5	93°10′13.08	6.5
92°9′30.96	3	92°37′27.12	7.2	93°3′41.4	3.5	93°10′17.4	9
92°12′11.88	3	92°38′55.68	6.5	93°4′4.8	4.5	93°10′24.6	7
92°13′3	2.5	92°39′14.04	7.5	93°4′24.96	5	93°10′26.76	7
92°13′26.04	3.5	92°39′28.8	7	93°4′28.56	6	93°11′3.48	4
92°16′46.92	3	92°39′29.88	8.6	93°4′42.24	7	93°11′46.68	4.5
92°17′0.96	3	92°41′28.68	5.1	93°5′3.48	7.5	93°12′25.2	4.5
92°18′29.16	2.5	92°41′36.24	4.7	93°5′17.88	5	93°12′45	6
92°18′32.76	3	92°46′20.28	6.0	93°6′10.44	4	93°13′3	7
92°19′33.6	4	92°46′37.56	6.0	93°6′35.64	3.5	93°13′49.44	5
92°20′24	3	92°47′3.48	5.0	93°6′50.76	4	93°13′57.72	7
92°20′33.36	2.5	92°56′33.72	2.5	93°7′2.64	4.5		
92°21′56.16	4	92°56′51	3	93°7′54.48	2.5		
92°22′2748	4	92°57′47.16	3	93°8′5.64	4		
92°58′45.48	3	93°8′21.48	4				

quake and an overview of the different rupture styles from west to east. Our mapping of the rupture documents a unique example of large scale coseismic slip partitioning along the central stretch of the Kusai segment of the Kunlun fault. Evidence for previous events on both the normal and strike-slip strands suggests that such partitioning behavior maybe stable rather than transient. A slight 3° counterclockwise swing in the strike of the fault suffices to cause such partitioning (King *et al.*, 2005). The kilometer-size displacements of ancient moraines confirm that, from Buka Daban Feng to the Kunlun Pass, and probably since at least the end of the penultimate glacial maximum (~140 ka), the Kusai segment may have slipped at a rate similar to that constrained for the Holocene (Kidd and Molnar, 1988; Li *et al.*, 2005; Van der Woerd *et al.*, 2002b). A novel set of coseismic surface offset measurements has been obtained from the restoration of geomorphic piercing lines on the HRS images. Although this data set is restricted to the central part of the Kusai segment of the fault, it shows clear fluctuations, by a factor of ~3, of the slip function over distances on the order of 30 km that correlate well with InSAR results. From ~3 m in the west, slip increases to 8 m around E92°36′ along a linear stretch of the fault where partitioning is well established. Farther eastward, smaller sinistral slip amounts of 4 to 5 m, near E92°42′, characterize a fault stretch marked by the succession of three pull-apart basins located in left-stepping jogs of a less linear fault zone. Seismic inversion (Antolik *et al.*, 2004) shows that this relative minimum lies in between the sources of two high-energy pulses, probably owing to the greater complexity of the fault surface at depth. Superficial slip increases again eastward as the fault becomes more linear. This suggests that variations of the slip function at scales of tens of kilometers actually reflect first-order changes in fault geometry at the surface and at depth. Slip fluctuations of this kind, which reach up to 100% (see also over a shorter rupture length, McGill and Rubin, 1999), thus not only provide important information on the internal subsegmentation of the fault but should also be taken into account when considering slip-per-event estimates derived from paleoseismic studies. Clearly, matching trench results with surface offsets measured tens of kilometers away should be regarded as hazardous.

For most of its length, the main rupture of the Kokoxili earthquake follows a long-lived tectonic feature (Kidd and Molnar, 1988; Meyer *et al.*, 1998; Van der Woerd *et al.*, 2002b) but the onset and termination of the rupture veer into somewhat unexpected paths. In the west, the rupture appears to have started on a hitherto poorly mapped fault in the west Tayang Hu basin, rather than on faults southwest of this lake that show more prominent active topographic and geomorphic signatures (Fig. 2), and are in more direct connection with the Manyi earthquake fault (1997). Our field survey nevertheless demonstrates that the west Tayang restraining bend broke several times during the Holocene prior to the 2001 event. This illustrates the complexity of the west Kunlun fault horsetail between the Manyi and Jingyu faults (Fig. 1). In the east, the rupture also follows a surprising path, running parallel to the main Xidatan segment of the Kunlun fault for few kilometers without triggering rupture of this segment. Instead it continues unabated south of the Burhan Budai range, propagating along the Kunlun Pass fault, with a minor thrust component. Careful inspection of

HRS and Spot (pixel, 10 m) images (acquired after the earthquake) of the region immediately west of the Kunlun Pass shows that the Kusai and Xidatan segments have no clear connection but remain separated at the surface by a still significant, probably long-lived step. The main south-directed drainages that cross the Kunlun Pass fault east of the Golmud–Lhasa road show rapidly decreasing sinistral cumulative offsets toward the east. Immediately south of the Burhan Budai ice cap, much of the long-term geomorphic evidence suggests predominant thrusting in contrast with the mostly sinistral motion observed during the 2001 earthquake. This implies that the east-propagating sinistral rupture triggered by the 2001 Kusai Hu earthquake east of the Kunlun Pass may not reflect the most common type of event on the Kunlun Pass fault. Ruptures of this style alone cannot generate the steep topographic gradient and prominent thrust throw that characterize the south flank of the Burhan Budai range. Smaller Kusai Hu earthquake ruptures may generally end at the eastern extremity of the Kusai Hu segment. One reason the 2001 Kusai Hu segment rupture did not continue along the Xidatan segment of the Kunlun fault may be related to the supershear rupture velocity (Bouchon and Vallée, 2003). In such a circumstance, the dynamic stress field ahead of the rupture front is strongly asymmetric (Poliakov *et al.*, 2002; Kame *et al.*, 2003) with a stress shadow north of the fault and a stress increase south of it promoting easier rupture along the Kunlun Pass fault. The lack of an established surface connection between the Kusai Hu and Xidatan segments of the fault suggests that rupture of the Kusai segment rarely continues along Xidatan in the same event. The Xidatan–Dongdatan segment is currently one of the last ones not to have ruptured along the western part of the Kunlun fault in the last few hundred years and is probably very close to failure (Li *et al.*, 2005; Van der Woerd *et al*., 2002b). The region just west of the Kunlun Pass is the place where the Kunlun fault penetrates into the Kunlun range instead of following its southern edge, as farther west. It would seem that a place where the rupture has to break across metamorphic rock (Li *et al.*, 2005) is likely to form a particularly deep and strong structural asperity capable of surviving scores of great earthquake seismic cycles.

Acknowledgments

This work was supported in France by the Institut National des Sciences de l'Univers/Centre National de la Recherche Scientifique (INSU-CNRS) and the Association Franco-Chinoise pour la Recherche Scientifique et Technique (AFCRST) and in China by the Chinese Earthquake Administration (CEA) Institute of Geology for the fieldwork. We are very indebted to Z. Chang from the CEA, Bureau of Golmud City, for his constant help to solve logistic issues. D. Bowman and W. Ma provided help and insight during the field operation. We thank G. Hilley and an anonymous reviewer for helpful reviews. The acquisition of the HRS images was possible due to support from Action Concertée Incitative (ACI) "Observation de la Terre" of INSU and the data purchase program of NASA. This article is IPGP contribution number 2062 and INSU contribution number 385.

References

Allen, C. R., L. Zhuoli, Q. Hong, W. Xueze, Z. Huawei, and H. Weishi (1991). Field study of a highly active fault zone: the Xianshuihe fault of southwestern China, *Geol. Soc. Am. Bull.* **103,** 1178–1199.

Antolik, M., R. E. Abercrombie, and G. Ekstrom (2004). The 14 November 2001 Kokoxili (Kunlunshan), Tibet, earthquake: rupture transfer through a large extensional step-over, *Bull. Seism. Soc. Am.* **94,** no. 4, 1173–1194.

Armijo, R., P. Tapponnier, J. L. Mercier, and H. Tong-Lin (1986). Quaternary extension in southern Tibet: field observations and tectonic implications, *J. Geophys. Res.* **91,** no. B14, 13,803–13,872.

Armijo, R., P. Tapponnier, and H. Tong-Lin (1989). Late Cenozoic right-lateral faulting in southern China, *J. Geophys. Res.* **94,** no. B3, 2787–2838.

Bhat, H., R. Dmowska, J. Rice, and N. Kame (2004). Dynamic slip transfer fromthe Denali to Totschunda faults, Alaska: testing theory for fault branching, *Bull. Seism. Soc. Am.* **94,** no. 6B, S202–S213.

Bouchon, M., and M. Vallée (2003). Observation of long supershear rupture during the $M_s = 8.1$ Kunlunshan earthquake, *Science* **301,** no. 5634, 824–826.

Bowman, D., G. King, and P. Tapponnier (2003). Slip partitioning by elastoplastic propagation of oblique slip at depth, *Science* **300,** 1121–1123.

Chevalier, M. L., F. J. Ryerson, P. Tapponnier, R. C. Finkel, J. Van der Woerd, H. B. Li, and Q. Liu (2005). Slip-rate measurements on the Karakorum fault may imply secular variations in fault motion, *Science* **307,** no. 5708, 411–414.

China Seismological Bureau (2002). *Album of the Kunlun Pass W. Ms = 8.1 Earthquake, China*, Seismological Press, Beijing China.

Fitch, T. J. (1970). Earthquake mechanisms in the Himalayan, Burmese, and Adaman regions and continental tectonics in central Asia, *J. Geophys. Res.* **75,** 2699–2709.

Gu, G., L. Tinghuang, and S. Zhenliang (1989). *Catalogue of Chinese Earthquakes (1831 BC–1969 AD)*, Science Press, Beijing, China.

Haeussler, P. J., D. P. Schwartz, T. E. Dawson, H. D. Stenner, J. J. Lienkaemper, B. Sherrod, F. R. Cinti, P. Montone, P. A. Craw, A. J. Crone, and S. F. Personius (2004). Surface rupture and slip distribution of the Denali and Totschunda faults in the 3 November 2002 *M* 7.9 earthquake, Alaska, *Bull. Seism. Soc. Am.* **94,** no. 6, S23–S52.

Jia, Y., H. Dai, and X. Su (1988). Tuosuo Lake earthquake fault in Qinghai Province, in *Research on Earthquake Faults in China*, X. S. Bureau (Editor), Xinjiang Press, Wurumuqi, 66–77.

Kame, N., J. R. Rice, and R. Dmowska (2003). Effects of prestress state and rupture velocity on dynamic fault branching, *J. Geophys. Res. Solid Earth* **108,** no. B5, 2265, doi 10.1029/2002JB002189, 2003.

Kidd, W. S. F., and P. Molnar (1988). Quaternary and active faulting observed on the 1985 Academia Sinica–Royal Society Geotraverse of Tibet, *Phil. Trans. R. Soc. London* **A327,** 337–363.

Kikuchi, M., and Y. Yamanaka (2001). *Special Event Page, 2001/11/14 Qinghai Xinjiang Border, China*, wwweic.eri.u-tokyo.ac.jp/topics/200111140926, Earthquake Information Center, ERI, Univ. Tokyo, Japan.

King, G., Y. Klinger, D. Bowman, and P. Tapponnier (2005). Slip partitioned surface breaks for the 2001 Kokoxili earthquake, China (M_w 7.8), *Bull. Seism. Soc. Am.* **95,** no. 2, 731–738.

Klinger, Y., K. Sieh, E. Altunel, A. Akoglu, A. Barka, T. Dawson, T. Gonzales, A. Meltzner, and T. Rockwell (2003). Paleoseismic evidence of characteristic slip on the western segment of the North Anatolian fault, Turkey, *Bull. Seism. Soc. Am.* **93,** no. 6, 2317–2332.

Lasserre, C., Y. Gaudemer, P. Tapponnier, A. S. Meriaux, J. Van der Woerd, D. Y. Yuan, F. J. Ryerson, R. C. Finkel, and M. W. Caffee (2002). Fast late Pleistocene slip rate on the Leng Long Ling segment of the Haiyuan fault, Qinghai, China, *J. Geophys. Res. Solid Earth* **107,** no. B11, 2276, doi 10.1029/2000JB000060, 2002.

Lasserre, C., G. Peltzer, Y. Klinger, J. Van der Woerd, and P. Tapponnier (2005). Coseismic deformation of the 2001 $M_w = 7.8$ Kokoxili earth-

quake in Tibet, measured by SAR interferometry, *J. Geophys. Res.* (in press).

Lasserre, C., G. Peltzer, J. Van der Woerd, Y. Klinger, and P. Tapponnier (2003). Coseismic deformation from the M_w = 7.8 Kokoxili, Tibet earthquake, from ERS InSAR data, *EGS EUG meeting (abstract)*, Nice, France, April 2003.

Le Pichon, A., J. Guilbert, M. Vallee, J. X. Dessa, and M. Ulziibat (2003). Infrasonic imaging of the Kunlun Mountains for the great 2001 China earthquake, *Geophys. Res. Lett.* **30,** no. 15, 1814, doi 10.1029/2003GL017581, 2003.

Li, H., J. Van Der Woerd, P. Tapponnier, Y. Klinger, X. Qi, J. Yang, and Y. Zhu (2005). Slip rate on the Kunlun Fault at Hongshui Gou, and recurrence time of great events comparable to the 14/11/2001, M_w ~7.9 Kokoxili earthquake, *Earth Planet. Sci. Lett.* (in press).

Li, L., and Y. Jia (1981). Characteristic of deformation band of the 1937 Tuosuohu earthquake (M=7.5) in Qinghai, *Northwest. Seis. J.* **3,** 61–65.

Lin, A., B. Fu, J. Guo, Q. Zeng, G. Dang, W. He, and Y. Zhao (2002). Co-seismic strike-slip and rupture length produced by the 2001 M_s 8.1 central Kunlun earthquake, *Science* **296,** 2015–2017.

Lin, A. M., J. M. Guo, and B. H. Fu (2004). Co-seismic mole track structures produced by the 2001 M_s 8.1 Central Kunlun earthquake, China, *J. Struct. Geol.* **26,** no. 8, 1511–1519.

Lin, A. M., M. Kikuchi, and B. H. Fu (2003). Rupture segmentation and process of the 2001 M_w 7.8 central Kunlun, China, earthquake, *Bull. Seism. Soc. Am.* **93,** no. 6, 2477–2492.

Liu, J., Y. Klinger, K. Sieh, and C. Rubin (2004). Six similar sequential ruptures of the San Andreas fault, Carrizo Plain, California, *Geology* **32,** no. 8, 649–652.

McGill, S., and C. Rubin (1999). Surficial slip distribution on the central Emerson fault during the June 28, 1992, Landers earthquake, *J. Geophys. Res.* **104,** no. B3, 4811–4834.

Meriaux, A. S., F. J. Ryerson, P. Tapponnier, J. Van der Woerd, R. C. Finkel, X. W. Xu, Z. Q. Xu, and M. W. Caffee (2004). Rapid slip along the central Altyn Tagh Fault: morphochronologic evidence from Cherchen He and Sulamu Tagh, *J. Geophys. Res. Solid Earth* **109,** no. B06401, doi 10.1029/2003JB002558, 2004.

Meyer, B., P. Tapponnier, L. Bourjot, F. Metivier, Y. Gaudemer, G. Peltzer, G. Shunmin, and C. Zhitai (1998). Crustal thickening in Gansu-Qinghai, lithospheric mantle subduction, and oblique, strike-slip controlled growth of the Tibet plateau, *Geophys. J. Int.* **135,** 1–47.

Ozacar, A. A., and S. Beck (2004). The 2002 Denali fault and 2001 Kunlun fault earthquakes: complex rupture processes of two large strike-slip events, *Bull. Seism. Soc. Am.* **94,** no. 6B, S278–S292.

Peltzer, G., F. Crampe, and G. King (1999). Evidence of nonlinear elasticity of the crust from the M_w 7.6 Manyi (Tibet) earthquake, *Science* **286,** 272–276.

Peyrat, S., K. Olsen, and R. Madariaga (2001). Dynamic modeling of the 1992 Landers earthquake, *J. Geophys. Res. Solid Earth* **106,** no. B11, 26,467–26,482.

Poliakov, A. N., R. Dmowska, and J. R. Rice (2002). Dynamic shear rupture interactions with fault bends and off-axis secondary faulting, *J. Geophys. Res.* **107,** no. B11, 6-1–6-18, doi 10.1029/2001JB000572.

Rice, J., C. G. Sammis, and R. Parsons (2005). Off-fault secondary failure induced by a dynamic slip-pulse, *Bull. Seism. Soc. Am.* **95,** 109–134.

Rivera, L., J. Van Der Woerd, A. Topechort, Y. Klinger, and C. Lasserre (2003). The Kokoxili, November 14, 2001, earthquake: history and geometry of the rupture from teleseismic data and field observations, *EGS-AGU-EUG Joint Assembly*, Nice, France, April 2003.

Scholz, C. (1990). *The Mechanics of Earthquakes and Faulting*, Cambridge University Press, New York.

Sieh, K. (1996). The repetition of large-earthquake ruptures, *Proc. Natl. Acad. Sci. U.S.A.* **93,** 3764–3771.

Tapponnier, P., and W. F. Brace (1976). Development of stress induced microcracks in Westerly granite, *Int. J. Rock. Mech. Min. Sci.* **13,** 103–112.

Tapponnier, P., and P. Molnar (1977). Active faulting and tectonics in China, *J. Geophys. Res.* **82,** 2905–2930.

Tapponnier, P., and J. Varet (1974). La zone de Mak'Arrosou en Afar: un equivalent émergé des failles transformantes océaniques, *CR Acad. Sci.* **278,** 209–212.

Tapponnier, P., X. Zhiqin, F. Roger, B. Meyer, N. Arnaud, G. Wittlinger, and Y. Jingsui (2001). Oblique stepwise rise and growth of the Tibet plateau, *Science* **294,** 1671–1677.

Tchalenko, J. S. (1970). Similarities between shear zones of different magnitudes, *Geol. Soc. Am. Bull.* **81,** 1625–1640.

Tchalenko, J. S., and N. Ambraseys (1970). Structural analysis of the Dasht-e Bayaz (Iran) earthquake fractures, *Geol. Soc. Am. Bull.* **81,** 41–60.

Van der Woerd, J., A. S. Meriaux, Y. Klinger, F. J. Ryerson, Y. Gaudemer, and P. Tapponnier (2002a). The 14 November 2001, M_w = 7.8 Kokoxili earthquake in northern Tibet (Qinghai Province, China), *Seism. Res. Lett.* **73,** no. 2, 125–135.

Van der Woerd, J., F. J. Ryerson, P. Tapponnier, Y. Gaudemer, R. Finkel, A. S. Meriaux, M. Caffee, G. Zao, and Q. He (1998). Holocene left slip-rate determined by cosmogenic surface dating on the Xidatan segment of the Kunlun fault (Qinghai, China), *Geology* **26,** 695–698.

Van der Woerd, J., F. J. Ryerson, P. Tapponnier, A. S. Meriaux, Y. Gaudemer, B. Meyer, R. Finkel, M. Caffee, G. Zhao, and Z. Xu (2000). Uniform slip-rate along the Kunlun fault: implication for seimic behaviour and large-scale tectonics, *Geophys. Res. Lett.* **27,** 2353–2356.

Van der Woerd, J., P. Tapponnier, F. J. Ryerson, A. S. Meriaux, B. Meyer, Y. Gaudemer, R. C. Finkel, M. W. Caffee, G. G. Zhao, and Z. Q. Xu, (2002b). Uniform postglacial slip-rate along the central 600 km of the Kunlun Fault (Tibet), from Al-26, Be-10, and C-14 dating of riser offsets, and climatic origin of the regional morphology, *Geophys. J. Int.* **148,** no. 3, 356–388.

Van der Woerd, J., X. W. Xu, H. B. Li, P. Tapponnier, B. Meyer, F. J. Ryerson, A. S. Meriaux, and Z. Q. Xu (2001). Rapid active thrusting along the northwestern range front of the Tanghe Nan Shan (western Gansu, China), *J. Geophys. Res. Solid Earth* **106,** no. B12, 30,475–30,504.

Velasco, A. A., C. J. Ammon, and S. Beck (2000). Broadband source modeling of the November 8, 1997 Tibet (M_w = 7.5) earthquake and its source implications, *J. Geophys. Res.* **105,** 28,065–28,028.

Vergne, J., G. Wittlinger, Q. Hui, P. Tapponnier, G. Poupinet, J. Mei, G. Herquel, and A. Paul (2002). Seismic evidence for stepwise thickening of the crust across the NE Tibatan plateau, *Earth Planet. Sci. Lett.* **203,** 25–33.

Wang, Q., P. Zhang, J. T. Freymueller, R. Bilham, K. M. Larson, X. Lai, X. You, Z. Niu, J. Wu, Y. Li, J. Liu, Z. Yang, and Q. Chen (2001). Present-day crustal deformation in China constrained by global positioning system measurements, *Science* **294,** 574–577.

Ward, S. (1997). Dogtails versus rainbows: synthetic earthquake rupture models as an aid in interpreting geological data, *Bull. Seism. Soc. Am.* **87,** 1422–1441.

Wittlinger, G., P. Tapponnier, G. Poupinet, J. Mei, S. Danian, G. Herquel, and F. Masson (1998). Tomographic evidence for localized lithospheric shear along the Altyn Tagh fault, *Science* **282,** 74–76.

Wittlinger, G., J. Vergne, P. Tapponnier, V. Farra, G. Poupinet, M. Jiang, H. Su, G. Herquel, and A. Paul (2004). Teleseismic imaging of subducting lithosphere and Moho offsets beneath western Tibet, *Earth Planet. Sci. Lett.* **221,** no. 1-4, 117–130.

Xu, X., W. Chen, W. Ma, G. Yu, and G. Chen (2002). Surface rupture of the Kunlunshan earthquake (M_s 8.1), northern Tibetan plateau, China, *Seism. Res. Lett.* **73,** no. 6, 884–892.

Laboratoire de Tectonique – UMR7578
Institut de Physique du Globe
4 place Jussieu
75005 Paris, France
klinger@ipgp.jussieu.fr
tappon@ipgp.jussieu.fr
king@ipgpjussieu.fr
(Y.K., P.T., G.K.)

Institut of Geology, CEA
Beijing 100029, China
xiweixu@vip.sina.com
(X.X.)

UMR7516, EOST, 5 r. Descartes
67000 Strasbourg, France
jeromev@eost.u-strasbg.fr
(J.V.)

Department of Earth and Space Sciences, UCLA
Los Angeles, California
lasserre@geologie.ens.fr
(C.L.)

Manuscript received 12 March 2004.